Highly Differentiated Human Fetal RPE Cultures Are Resistant to the Accumulation and Toxicity of Lipofuscin-Like Material

Qitao Zhang,[1] Feriel Presswalla,[1] Melissa Calton,[2] Carol Charniga,[3] Jeffrey Stern,[3] Sally Temple,[3] Douglas Vollrath,[2] David N. Zacks,[1] Robin R. Ali,[1,4] Debra A. Thompson,[1] and Jason M. L. Miller[1]

[1]Kellogg Eye Center, University of Michigan, Ann Arbor, Michigan, United States
[2]Department of Genetics, Stanford University School of Medicine, Stanford, California, United States
[3]Neural Stem Cell Institute, Rensselaer, New York, United States
[4]UCL Institute of Ophthalmology, London, United Kingdom

Correspondence: Jason M. L. Miller, Kellogg Eye Center, University of Michigan, 1000 Wall Street, Ann Arbor, MI 48105, USA; miljason@med.umich.edu.

Submitted: January 27, 2019
Accepted: July 17, 2019

Citation: Zhang Q, Presswalla F, Calton M, et al. Highly differentiated human fetal RPE cultures are resistant to the accumulation and toxicity of lipofuscin-like material. *Invest Ophthalmol Vis Sci*. 2019;60:3468–3479. https://doi.org/10.1167/iovs.19-26690

Purpose. The accumulation of undigestible autofluorescent material (UAM), termed lipofuscin in vivo, is a hallmark of aged RPE. Lipofuscin derives, in part, from the incomplete degradation of phagocytized photoreceptor outer segments (OS). Whether this accumulated waste is toxic is unclear. We therefore investigated the effects of UAM in highly differentiated human fetal RPE (hfRPE) cultures.

Methods. Unmodified and photo-oxidized OS were fed daily to confluent cultures of ARPE-19 RPE or hfRPE. The emission spectrum, composition, and morphology of resulting UAM were measured and compared to in vivo lipofuscin. Effects of UAM on multiple RPE phenotypes were assessed.

Results. Compared to ARPE-19, hfRPE were markedly less susceptible to UAM buildup. Accumulated UAM in hfRPE initially resembled the morphology of lipofuscin from AMD eyes, but compacted and shifted spectrum over time to resemble lipofuscin from healthy aged human RPE. UAM accumulation mildly reduced transepithelial electrical resistance, ketogenesis, certain RPE differentiation markers, and phagocytosis efficiency, while inducing senescence and rare, focal pockets of epithelial-mesenchymal transition. However, it had no effects on mitochondrial oxygen consumption rate, certain other RPE differentiation markers, secretion of drusen components or polarity markers, nor cell death.

Conclusions. hfRPE demonstrates a remarkable resistance to UAM accumulation, suggesting mechanisms for efficient OS processing that may be lost in other RPE culture models. Furthermore, while UAM alters hfRPE phenotype, the effects are modest, consistent with conflicting reports in the literature on the toxicity of lipofuscin. Our results suggest that healthy RPE may adequately adapt to and tolerate lipofuscin accumulation.

Keywords: lipofuscin, macular degeneration, retinal pigment epithelium, cell culture model

The daily ingestion of shed OS tips from photoreceptors by the RPE is critical for photoreceptor health and function. As the RPE is a mostly postmitotic tissue, the phagocytic burden for each cell over a lifetime is immense. Incomplete degradation of OS material contributes, in part, to the development of autofluorescent intracellular inclusions termed lipofuscin.[1] Lipofuscin accumulates over a lifetime, occupying major portions of the RPE cell in elderly individuals.[2–4] It contains numerous components, including a complex mixture of bisretinoids derived from covalent linkage of monoretinoids used in the visual cycle, oxidized lipid products, and cross-linked protein.[5] Whether this accumulated waste is toxic to the RPE, and in what diseases, is heavily debated.[6,7] In support of lipofuscin toxicity, animal models lacking the ABCA4 gene, mimicking the defect seen in Stargardt disease, accumulate lipofuscin at an accelerated rate and demonstrate retinal degeneration.[8] Numerous components of lipofuscin, in particular the bisretinoid N-retinylidene-N-retinylethanolamine (A2E), have been shown in cell culture and animal models to dysregulate complement activity, induce photo-oxidative damage, and disrupt lysosomal integrity.[9,10] On the other hand, lipofuscin-related fundus autofluorescence from patients with early- or intermediate-stage AMD is no higher than age-matched controls.[6] Further, the concentration of A2E or its oxidized components is no higher in RPE underlying the macula compared to the retinal periphery, despite AMD being a macular disease.[11] Additionally, there is minimal evidence supporting a link between lipofuscin and the pathologic hallmark of AMD, extracellular accumulation of lipid-rich deposits above (termed reticular pseudodrusen) and below (termed drusen) the RPE; while lipofuscin accumulates in the RPE of all persons as they age, only a subset develop pathologic drusen or reticular pseudodrusen. While levels of lipofuscin may not correlate with drusen formation or retinal toxicity, the lipofuscin granules in patients with AMD have been reported to be larger and more irregular than granules simply associated with age.[3] The significance of this difference is unknown.

Distinguishing whether lipofuscin is toxic in AMD patients in the clinic is difficult. As RPE cells die, lipofuscin is lost and fundus autofluorescence decreases. Thus, any degree of cell death decreases the strength of any putative relationship between lipofuscin and toxicity. Prior to RPE cell death, the marked accumulation of lipofuscin in normal, healthy, aged RPE creates a strong "background" above which any disease-specific signal is difficult to measure. To understand the relationship between lipofuscin and RPE toxicity in a more controlled setting, a number of groups have attempted to model lipofuscin accumulation in cell culture. Many groups have fed a single bisretinoid, A2E, to the RPE cultures.[12–14] However, controversy exists over which, if any, specific bisretinoids are toxic.[1,15] Furthermore, it may not be possible to recapitulate an accurate model of lipofuscinogenesis by feeding RPE with just one type of bisretinoid. An alternate approach is to induce lipofuscinogenesis by OS feedings of cultures.[1,16] However, this has not been done in primary (passage 1) human fetal RPE (hfRPE) cultures, among the most extensively validated systems for in vitro studies of human RPE.[17] Here, we develop a model for accumulation of lipofuscin-like material, which we term undigested autofluorescent material (UAM), in hfRPE cultures through repeated OS feedings.

We discovered that UAM granules are dynamic, compacting and shifting their spectrum over time, suggesting that newly formed and older granules may have different biologic effects. Newer granules resembled those seen in RPE from patients with AMD; older granules more closely resembled lipofuscin from healthy, aged patients. While hfRPE cultures were remarkably resistant to UAM accumulation, cultures with heavy UAM burden had mild defects in tight-junction integrity, ketogenesis, RPE differentiation, and phagocytic capacity. The cultures also demonstrated increased senescence and rare, focal pockets of transition from an epithelial to mesenchymal phenotype. Nevertheless, UAM-laden hfRPE cultures exhibited no alteration in oxygen consumption rate, a marker of mitochondrial health, secretion of drusen components, cell polarity, expression of certain other RPE differentiation markers, or rates of cell death. The resistance of hfRPE to UAM accumulation, combined with only modest effects of UAM on hfRPE function, suggest that highly-differentiated and healthy RPE are adaptable to lipofuscin accumulation.

Methods

ARPE-19, Primary hfRPE, and Primary ahRPE Culture

ARPE-19 cells were obtained from the Hjelmeland laboratory[18] at passage 18 and split from confluency at a ratio of 1:3 onto porous cell culture inserts (Corning 24-well Transwells, #7200154; Thermo Fisher Scientific, Waltham, MA, USA), incubated in "RPE media" (see hfRPE cultures below) for at least 12 weeks prior to use in experiments. hfRPE was cultured as we described.[19] Step-by-step directions for our hfRPE culture are available at https://medicine.umich.edu/sites/default/files/content/downloads/Human_RPE_Culture_Protocol.pdf. Passage 1 hfRPE cells were in culture on Transwells for at least 2 months prior to experimentation. ahRPE primary cultures were established from human adult retinal pigment epithelial stem cells derived from cadaver eyes from healthy donors, grown as passage 1 on 24-well Transwells according to methods previously published,[20,21] and, once established on Transwells for at least 4 weeks, switched to the same RPE media used for hfRPE cultures ("RPE media"). ahRPE were in culture for at least 3 to 4 months after Transwell plating prior to being used for experiments.

UAM Buildup

Bovine outer segments were isolated as described.[19] Step-by-step directions for our isolation protocol are available at https://medicine.umich.edu/sites/default/files/content/downloads/Photoreceptor_Outer_Segment_Isolation.pdf. To photooxidize OS, 500 µl of 1×10^8 OS/mL was pipetted onto Teflon-masked microscope slides (three rectangles per slide, measuring 17 × 9 mm; Tekdon, Myakka, FL, USA), and illuminated at 254 nm at an estimated radiant exposure of 3J/cm^2 for 40 minutes. oxOS were then pelleted and resuspended in hfRPE medium at 5.6×10^7 OS/mL. In certain cases, purified MFG-E8 (#10853-H08B; Sino Biological, Wayne, PA, USA) at 4.2 µg/mL and protein S (#HPS; Enzyme Research Laboratories, South Bend, IN, USA) at 11.2 µg/mL were added to the oxOS suspension. Aliquots were flash frozen in liquid nitrogen and stored until use at –80°C.

To induce UAM, 25 µl oxOS aliquots were added to 45 µl of fresh RPE media for each 24-well Transwell. Total apical Transwell volume was 70 µL, and final concentration was 2×10^7 oxOS/mL, 1.5 µL MFG-E8/mL, and 4 µL Protein S/mL. Control wells were either fed regular OS (RegOS) under identical conditions or were fed 25 µl of flash-frozen media combined with 45 µL of fresh RPE media (media). oxOS, RegOS, or media feedings occurred 5 times per week for a total of 4 weeks unless otherwise specified.

Measuring UAM

Autofluorescence from UAM-laden RPE cultures was measured using a confocal microscope (Leica SP5; Leica Microsystems, Buffalo Grove, IL, USA). At the conclusion of oxOS feedings, oxOS were washed 3 times with PBS without calcium or magnesium and subsequently left in RPE media for at least 1 week prior to experimentation. This additional "chase" period resulted in a dramatic reduction in surface-bound autofluorescent OS, which otherwise confounds determination of UAM autofluorescence. For quantification of UAM, we stained cultures with anti-rhodopsin antibody (#MCA-B630; Encor Biotech, Gainesville, FL, USA) without permeabilization, leading to specific labeling of any remaining autofluorescent surface-bound OS. We then applied the anti-rhodopsin fluorescence channel as a subtractive mask on the autofluorescence channel to quantify autofluorescence specifically from UAM. Quantification was carried out using commercial software (Imaris; Bitplane, Concord, MA, USA).

Phagocytosis Assays

OS consumption was determined using the "pulse-only" method outlined previously,[19] followed by PAGE and blotting with MCA-B630[22] +/– 1D4[23] anti-rhodopsin antibodies.

OS Compositional Analysis

OS were separated into protein and lipid-rich fractions using chloroform/methanol extraction, based on modifications to the original procedure.[24] OS (1×10^8) were pelleted, homogenized in 600 µL of 1:2 ice-cold chloroform/methanol, incubated on ice for 3 minutes, and sonicated. We added 200 µL of chloroform and 255 µL of water, the lower phase (chloroform) was removed, and the extraction was repeated twice. Chloroform fractions were dried under argon flow and resuspended in hexane. The precipitated protein fraction was removed from the methanol/water phase. The fractions were dried on a microscope slide and subjected to spectral analysis on a confocal microscope (SP5 Leica; Leica Micro-

Investigative Ophthalmology & Visual Science

systems) using 405-nm excitation and the microscope's spectral detection filter (lambda scan).

UAM Compositional Analysis

Emission spectra of UAM were performed using 405-, 458-, or 488-nm excitation and the confocal microscope's (Leica SP5; Leica Microsystems) lambda scan detectors. Probing UAM for rhodopsin utilized antibody MCA-B630. Nile Red (10 μg/mL) was incubated for 30 minutes followed by 5X PBS wash. During imaging, controls containing UAM without Nile Red were used to determine the contribution of autofluorescence to the Nile Red channel.

Transmission electron microscopy was performed on Transwell membranes cut free from the Transwell, fixed in 2.5% glutaraldehyde overnight, rinsed in PBS, and postfixed for 1 hour at RT with 1% osmium tetroxide. After another PBS rinse, the membrane was dehydrated for 5 minutes each in 25, 50, 70, 98, and then 2X 100% acetone. The membrane was embedded in Embed 812 resin, polymerized at 60°C for 24 hours, and sectioned on an ultra-microtome. Sections were stained with uranyl acetate and lead citrate, then imaged on a transmission electron microscope (JEOL-JEM 1400 Plus; JEOL, Peabody, MA, USA).

Measuring TEER and Cell Death

TEER was measured with a volt-ohmmeter and electrode probe (EVOM and STX2; World Precision Instruments, Sarasota, FL, USA). Details on obtaining reproducible resistance readings are available at: https://medicine.umich.edu/sites/default/files/content/downloads/Measuring_Transepithelial_Electrical_Resistance.pdf.

Cell death was measured on cultures at least several weeks after last OS feeding using a cytotoxicity assay (LDH-Glo, #J2380; Promega, Madison, WI, USA) according to manufacturer's instructions. Supernatant (24-hour incubation) was diluted 1:100, and 50 μL of the dilution was measured on a luminometer (Veritas; Promega), subtracting all values from the signal derived from fresh media.

Seahorse Analysis

hfRPE were plated as intact monolayers on Transwell membranes in XFp cell culture miniplate wells (#103022–100; Agilent, Santa Clara, CA, USA), and cellular energetics were measured as described.[25] Briefly, triangular inserts were cut from 24-well Transwells approximately 3 weeks after last oxOS feeding and placed in the XFp cell culture miniplate. Cells were incubated for 60 minutes in medium (XF Assay Medium, #103334–100; Agilent Technologies, Santa Clara, CA, USA) supplemented with 5.5 mM glucose, 1 mM sodium pyruvate, and 2 mM L-glutamine. Background signal was measured from unseeded Transwells placed in the XFp cell culture miniplate. Three replicate miniplate wells (technical triplicates) were used for each Transwell. Oxygen consumption rate (OCR), an indicator of mitochondrial respiration, and the extracellular acidification rate (ECAR), an indicator of aerobic glycolysis, were measured on three sequential timepoints (additional technical replicates) using a commercial analyzer (Seahorse XFp; Agilent Technologies). Cells were then trypsinized using 0.25% trypsin-EDTA and counted using a hemocytometer. Each well was normalized to the number of cells counted after the run.

Given multiple technical and biological replicates, we employed mixed effects regression for statistical analysis, designating UAM as the fixed effect and well replicate, time replicate, and donor as random effects. Analyses were performed in R 3.5.1 (www.R-project.org) using the lmer() function of the lme4 package[26] to design a linear mixed effects model fit by maximum likelihood. Comparisons of means (+/− lipofuscin for ECAR and for OCR) were performed on the modeled data using the glht() function in the multcomp package.[27]

Secretion and Polarity Analysis

After incubating Transwells in 200 μL of RPE media both apically and basolaterally for 24 hours, 50 μL of supernatant from each side of the Transwell was analyzed using a commercial assay kit (Amplite Fluorimetric Beta-Hydroxybutyrate, #13831; AAT Bioquest, Sunnyvale, CA, USA) according to manufacturer's instructions. Standard curves were created using RPE media. Signal was read 20 minutes after mixing, using a luminometer (Promega).

ApoE, TIMP3, and PEDF secretion were measured from Transwells also incubated with 200 μL RPE media apically and basolaterally. Media was collected after a 72-hour incubation for ApoE and after a 24-hour incubation for TIMP3 and PEDF. A supernatant volume of 7.5 μL per well was subjected to PAGE and blotted with anti-ApoE (#AB947, Millipore Corp., Burlington, MA, USA), anti-TIMP3 (#AB6000, Millipore Corp.), or anti-PEDF (#AB180711; Abcam, Cambridge, UK).

Senescence, EMT, and RPE-Specific Gene Analysis

Senescence of hfRPE was measured on paraformaldehyde-fixed cultures after completion of oxOS feeding, using beta-galactosidase staining according to manufacturer's instructions (#9860; Cell Signaling Technology, Danvers, MA, USA). Paraformaldehyde-fixed cultures were subjected to anti-vimentin antibody (#OMA1-06001, Thermo Fisher Scientific). EMT and RPE-specific gene markers were measured by qPCR (CFX 384 rtPCR thermocycler; Bio-Rad Laboratories, Hercules, CA, USA) as previously described,[19] using primers to Slug (Slug-F:5′-CATGCCTGTCATACCACAAC-3′ and Slug-R:5′-GGTGTCA GATGGAGGAGGG-3′)[28] and Twist1 (Twist1-F:5′-CACTGAAAG GAAAGGCATCA-3′ and Twist1-R:5′-GGCCAGTTTGATCCCAG TAT-3′)[29] for EMT. RPE-specific gene primers included RPE65 (RPE65-F:5′-CGTCATAACAGAATTTGGCACC-3′ and RPE65-R:5′-GCCCCATTGACAGAGACATAG-3′),[19] CRALBP (CRALBP-F:5′-CTGGCAAAGTCAAGAAATCAC-3′ and CRALBP-R:5′-TGTC CACCATCTTCCTGAG-3′),[19] BEST1 (BEST1-F:5′-TTGGAGGTC GAATCCGGGA-3′ and BEST1-R:5′-GTCCACACTGAGTACG CAAGG-3′; PrimerBank ID 212720874c3, pga.mgh.harvard.edu/primerbank/index.html), TIMP3 (TIMP3-F:5′-CATGTG CAGTACATCCATACGG-3′ and TIMP3-R:5′-CATCATAGACGC GACCTGTCA-3′),[30] and CLDN19 (CLDN19-F:5′-CTCAGCGTAG TTGGCATGAA-3′ and CLDN19-R:5′-GAAGAACTCCTGGGT CACCA-3′).[31] β-actin (β-actin-F:5′-CAGGATGCAGAAGGAGAT CAC-3′ and β-actin-R:5′-TGTCAAGAAAGGGTGTAACGC-3′)[19] was used as a normalization control.

Statistical Analysis

For experiments with outcomes measured in arbitrary units (e.g., fluorescence, luminescence), experimental replicates were normalized to each other using the average value for each experimental repeat. Means were compared using paired or unpaired Student's *t*-tests, as appropriate. All error bars represent standard error of the mean.

Results

Previous studies have shown the accumulation of UAM after a few weeks of OS feeding in RPE cell lines or primary RPE

Investigative Ophthalmology & Visual Science

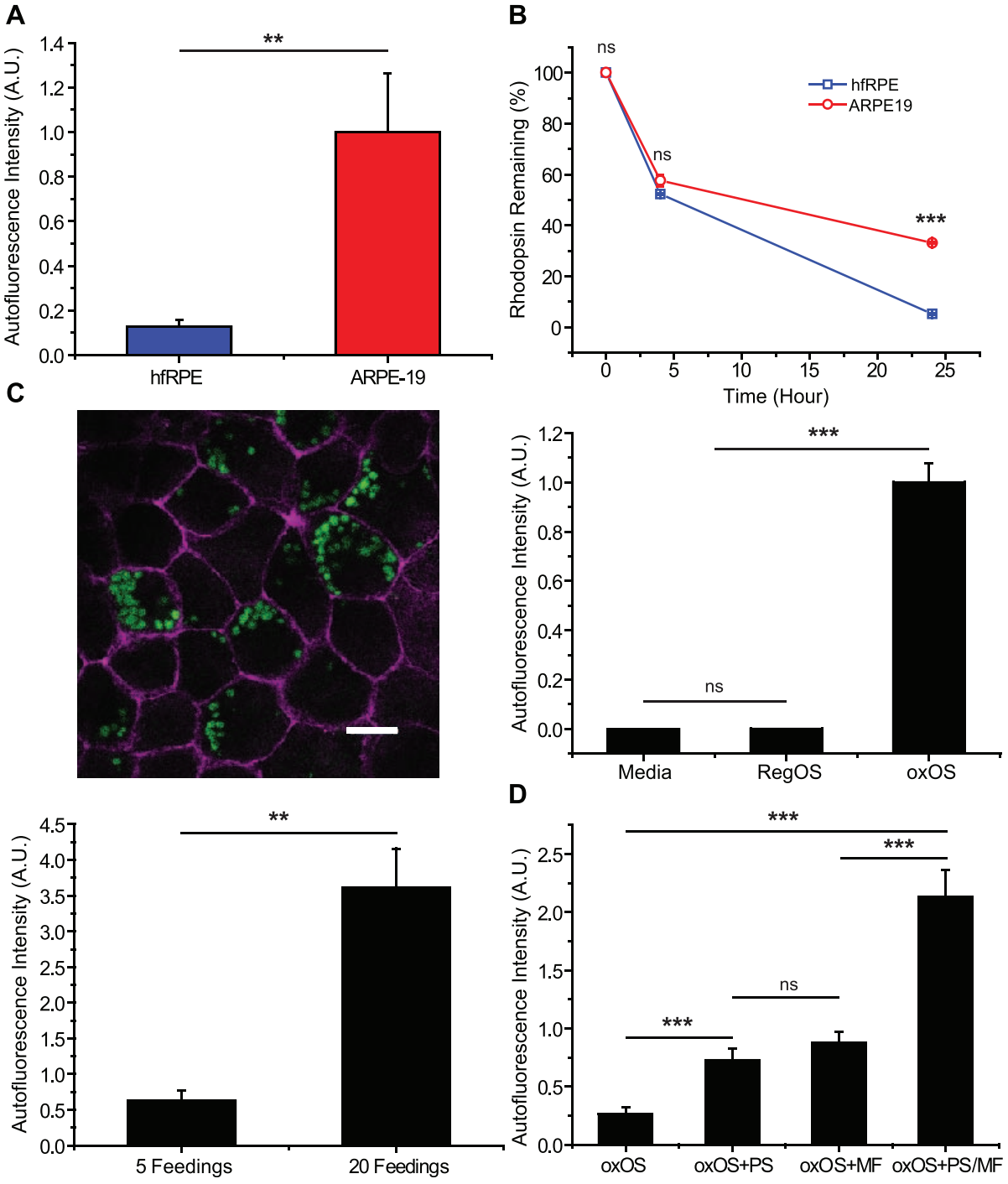

Figure 1. hfRPE cultures are resistant to UAM accumulation. UAM imaged with 488-nm excitation and 500 to 535 nm emission. **(A)** Fourteen daily RegOS feedings with PS and MFG-E8 (MF) produced UAM in ARPE-19 cultures but not hfRPE cultures; $n = 6$. **(B)** Consumption of an OS bolus, as measured by rhodopsin remaining, is greater in hfRPE than ARPE-19 cultures; $n = 3$. **(C)** Fourteen daily oxOS feedings with PS and MF, but not with media only or RegOS feedings, produced UAM in hfRPE cultures. UAM accumulation was dose-dependent (5 versus 20 daily oxOS feedings). Micrograph: UAM autofluorescence (*green*) and CF647-conjugated phalloidin stain of actin (*purple*). *Scale bar*: 10 µm. $n = 26$ for media versus RegOS versus oxOS graph. $n = 6$ for dose-response graph. **(D)** UAM accumulation is phagocytosis-dependent. Accumulation markedly increases in the presence of phagocytosis bridging ligands PS and MF; $n = 17$. ns, nonsignificant. $^{*}P < 0.05$, $^{**}P < 0.01$, $^{***}P < 0.001$.

cultures.[1,32–34] Sundelin and Nilsson[33] observed lipofuscin-like material after feeding primary rabbit RPE cultures outer segments every other day for 18 days. Boulton et al.[32] fed primary human adult RPE cultures with outer segments for 2 to 12 weeks, observing lipofuscin-like autofluorescence two weeks after initiation of feeding. Primary human adult RPE cultures from Zhang et al.[34] developed autofluorescence after four days of feeding. We therefore began by feeding hfRPE 14 consecutive daily boluses of purified bovine OS (regular OS: RegOS). We failed to observe any UAM, even using high concentrations of OS (2×10^7 OS/mL; ~15 OS/RPE cell; equal to or greater than previously published studies) augmented by

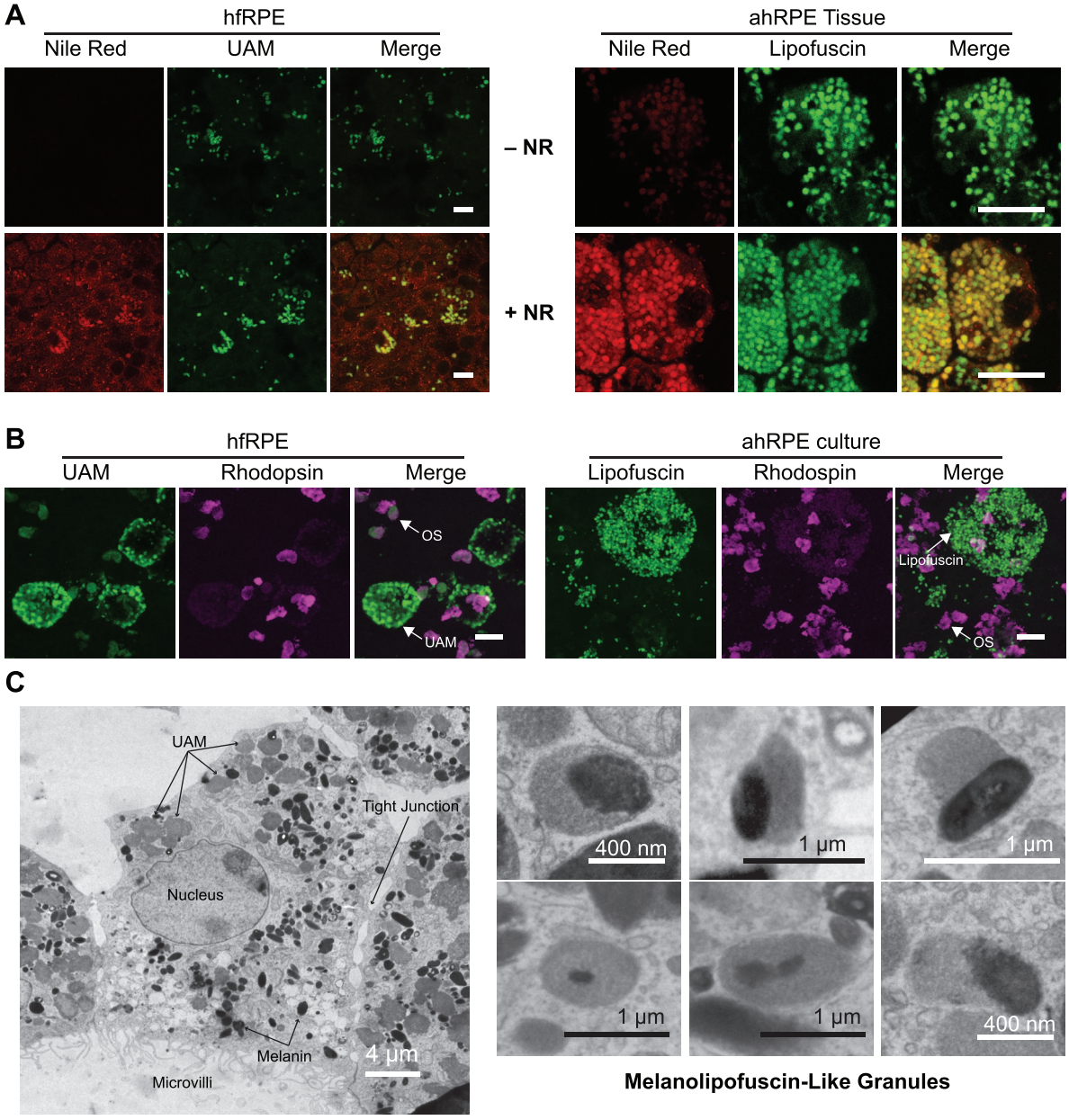

Figure 2. Composition of UAM. (**A**) Nile Red staining of neutral lipids associated with UAM in hfRPE (*left*) and in vivo lipofuscin in freshly isolated RPE tissue (ahRPE) from 69-year-old male with no ocular pathology (*right*). *Top row* is without Nile Red to control for any autofluorescence bleedthrough from UAM or lipofuscin into Nile Red channel. *Bottom row* is with Nile Red. *Scale bar*: 10 µm. (**B**) Rhodopsin staining is not associated with hfRPE UAM (*left*) or in vivo lipofuscin "carried-over" into P1 ahRPE primary cultures (*right*). Cultures were fed a single bolus of OS as a positive control to confirm rhodopsin staining and demonstrate intrinsic autofluorescence from OS. UAM/lipofuscin and OS autofluorescence (*green*), B630 anti-rhodopsin antibody (*purple*). *Scale bar*: 10 µm. (**C**) (*Left*) Electron micrograph of hfRPE fed photo-oxidized OS on 20 separate days over a 4-week period reveals a homogenous granular structure to the accumulated UAM, similar to in vivo lipofuscin. (*Right*) Higher magnification views from other cells show that certain granules contain a mixture of UAM and melanin, mimicking the appearance of melanolipofuscin in RPE from patients as they age.

addition of purified phagocytosis bridging ligands, human protein S (PS) and milk fat globulin E8 (MF) (Fig. 1A). We previously demonstrated that addition of these bridging ligands, which link phosphatidylserine moieties on OS membranes with the phagocytosis receptors αvβ5 integrin and Mer tyrosine kinase (MerTK) on the RPE apical membrane,[35] significantly improves total uptake of OS in our hfRPE culture system.[19] Even the addition of subtoxic doses (3.5–5 mM) of the lysosomal poison, ammonium chloride, with OS feedings, which greatly reduces complete OS breakdown in other RPE culture models,[36] failed to produce UAM in hfRPE (data not shown). In contrast, 2 weeks of daily RegOS feedings to ARPE-19 cells, a human RPE cell line, resulted in significant UAM (Fig. 1A), consistent with prior studies.[1] The differences in UAM accumulation between hfRPE and ARPE-19 cultures were not attributable to differences in the number of ingested OS, as hfRPE had a higher rate of outer segment consumption (Fig. 1B). These experiments demonstrate the special capacity of hfRPE to efficiently degrade OS, thereby minimizing UAM accumulation.

To induce UAM accumulation in hfRPE, we photo-oxidized outer segments (oxOS) using 254 nm UV light and fed these

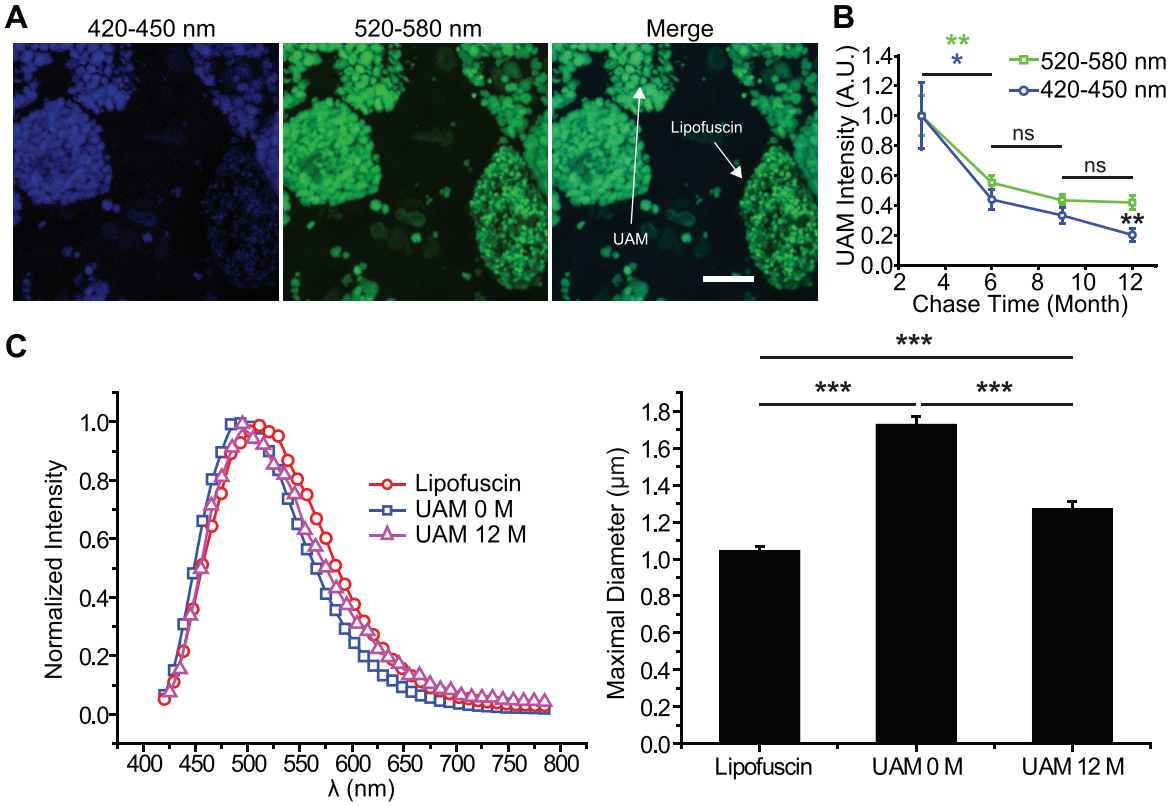

Figure 3. UAM granule spectrum and size evolve over time to more closely mimic in vivo lipofuscin. (**A**) UAM emission spectrum (405-nm excitation) is blue-shifted compared to carryover lipofuscin granules in ahRPE primary cultures that contain both types of granules. UAM granules are also larger than carryover lipofuscin granules. Images taken within 3 weeks of completing oxOS feedings. Autofluorescence emission simultaneously captured in blue channel (420–450 nm) and green channel (520–580 nm). *Scale bar*: 10 μm. (**B**) UAM persists for at least 1 year after last oxOS feeding. Over time, blue UAM autofluorescence (420–450 nm) declines more than the green UAM autofluorescence (520–580 nm), suggesting that UAM spectrum red-shifts when in culture for prolonged periods; 405 nm excitation. $n = 10$ from hfRPE cultures. *Blue* and *green asterisks* signify differences between 3 and 6 months for blue and green autofluorescence, respectively. The *blue* and *green curves* are statistically different from each other only at 12 months (*double asterisks*). (**C**) UAM emission spectrum (405-nm excitation) is initially blue-shifted compared to carry-over lipofuscin (0 M = 0 months), but this spectrum red-shifts over time to more closely resemble carry-over lipofuscin (12 M = 12 months). Concurrently, UAM granules compact over time, more closely resembling the size of carry-over lipofuscin. $n = 50$ from hfRPE cultures. $^{*}P < 0.05$, $^{**}P < 0.01$, $^{***}P < 0.001$.

oxOS 5 to 7 times per week to cultures for up to 4 weeks.[37] oxOS contained significantly more autofluorescence than RegOS, and this autofluorescence was distributed across both the protein and lipid fractions of the OS (Supplementary Fig. S1A). The autofluorescent emission spectrum (405-nm excitation) for oxOS was blue-shifted compared to RegOS, but the emission spectrum from the oxOS protein and lipid fractions were identical (Supplementary Fig. S1B). As expected, photooxidation triggered OS protein cross-linking (Supplementary Fig. S1C).

Feeding of oxOS to our hfRPE cultures induced UAM accumulation in a dose-dependent manner (Fig. 1C). UAM formation was also phagocytosis-dependent, as more UAM accumulated in the presence of protein S and MFG-E8 (Fig. 1D). To allow for direct comparison between UAM and endogenous human lipofuscin, we cultured passage 1 primary human adult RPE (ahRPE).[20] These adult cultures contain "carryover" lipofuscin granules that existed in vivo at the time of death and persist in low-passage culture. We also examined lipofuscin from RPE sheets freshly harvested from aged human eyes. Consistent with previous reports examining endogenous human lipofuscin[38] and our own examination of freshly isolated RPE from human donors and carry-over lipofuscin in ahRPE cultures, UAM in our hfRPE cultures contains neutral lipids (Fig. 2A) and is devoid of rhodopsin staining (Fig. 2B). By transmission electron microscopy, the granules also resemble the electron density and shape of in vivo lipofuscin. The fusion of melanosomes and lipofuscin granules into melanolipofuscin, a characteristic of in vivo aging, is also seen in our hfRPE model (Fig. 2C).[39–41]

UAM granules formed in ahRPE from RegOS feedings had the same emission spectrum (excitation: 458 nm) as UAM granules formed from oxOS feedings, suggesting a similar composition of UAM granules despite differences in chemical constituents of RegOS vs. oxOS (Supplementary Fig. S2). However, when compared to in vivo carryover lipofuscin in primary ahRPE cultures derived from donors without ocular pathology, UAM granules were larger with a blue-shifted emission spectrum (Fig. 3A). UAM granules persisted in culture for many months after oxOS feeding ended (Fig. 3B), but their spectrum and size shifted over time to more closely resemble endogenous age-related human lipofuscin (Figs. 3B, 3C).

Cultures of UAM-laden hfRPE were remarkably stable over time. Cultures experienced an initial drop in trans-epithelial electrical resistance (TEER), a marker of epithelial tight junction integrity, compared to hfRPE cultures fed RegOS or daily media changes (media), but this drop in TEER plateaued quickly and cultures were viable for months after UAM buildup (Fig. 4A). Additionally, we measured no significant increase in cell death after UAM-buildup, as assayed by lactate dehydroge-

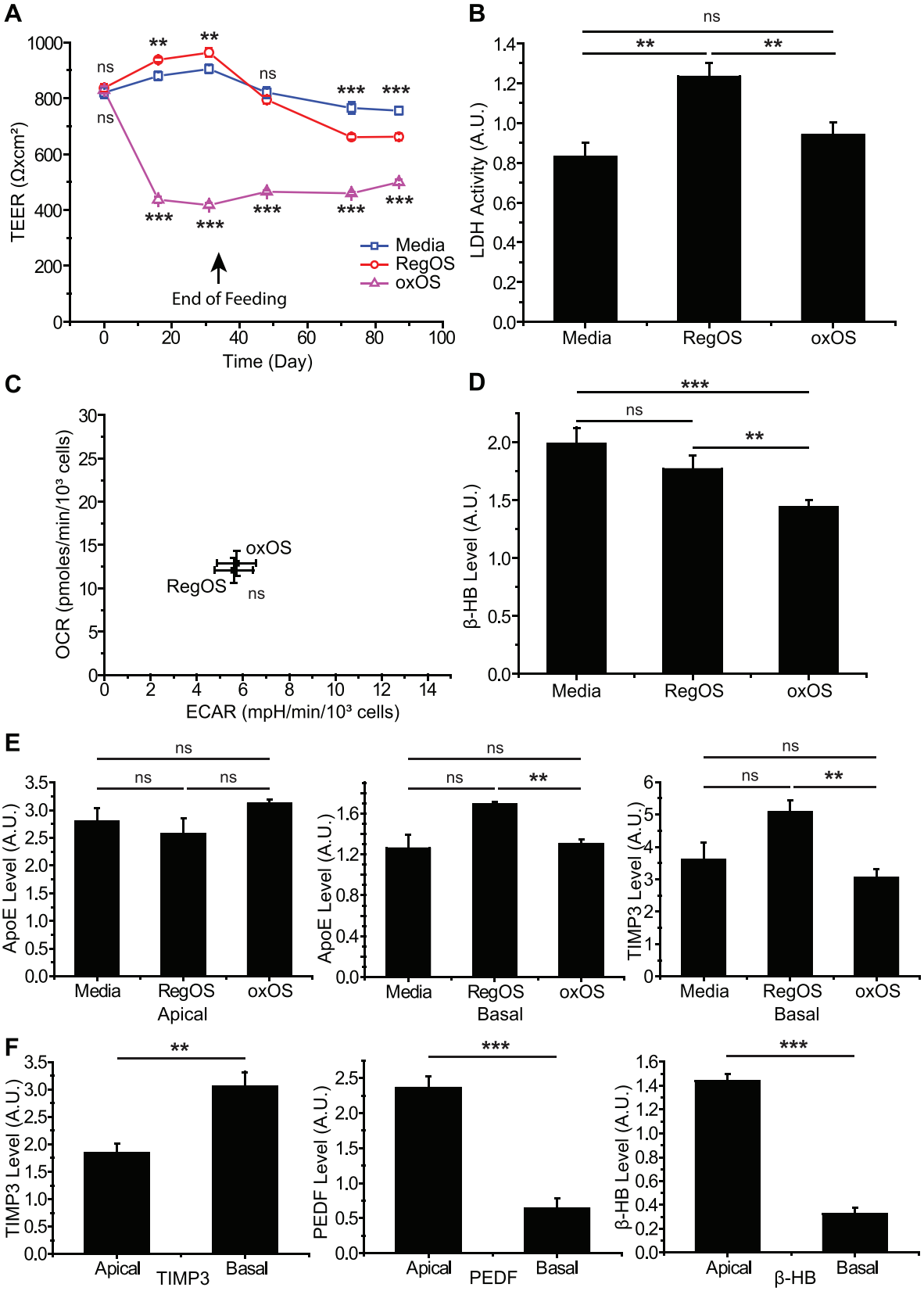

Figure 4. UAM-laden hfRPE cultures exhibit minimal toxicity. (**A**) Compared to cultures repeatedly fed RegOS or daily media changes, cultures fed oxOS demonstrate an initial drop in TEER. However, this drop stabilizes quickly, well before the end of oxOS feeding (*arrow*). $n = 12$. (**B**) Cell death, as assayed by LDH release, was no higher in UAM-laden cultures (fed oxOS) than those fed RegOS or media-only. Assay performed at least several weeks after last feeding; $n = 8$. (**C**) OCR and ECAR of hfRPE cultures with UAM (oxOS) and without UAM (RegOS) are not significantly different, suggesting oxidative phosphorylation and glycolysis are unaltered in hfRPE burdened with UAM. OCR and ECAR measured on confluent hfRPE on Transwells using modification to standard Seahorse Analyzer technique[25]; $n = 15$. (**D**) Ketogenesis is mildly diminished in UAM-laden cultures

(oxOS) compared to those fed RegOS or media only. Secreted β-hydroxybutyrate (β-HB) measured in the apical Transwell chamber several weeks after last OS or daily media feeding; $n = 16$. (**E**) Secretion of drusen components ApoE ($n = 3$) and TIMP3 ($n = 5$) are unaltered in hfRPE cultures with UAM (oxOS) compared to cultures fed daily media changes. Measurements taken several weeks after last feeding. (**F**) Polarity of UAM-laden hfRPE (oxOS) is well-preserved, as assessed by preferential basolateral secretion of TIMP3 ($n = 5$) and preferential apical secretion of PEDF ($n = 5$) and ketone bodies ($n = 16$). $^{**}P < 0.01$, $^{***}P < 0.001$.

nase release (Fig. 4B). Since lipofuscin involves storage in a modified lysosomal compartment and lysosomes are known to control cellular metabolism,[42] we also tested for UAM effects on glycolysis and mitochondrial capacity. Glycolysis can be measured via extracellular acidification (ECAR) and mitochondrial metabolism measured through oxygen consumption rates (OCR) using a Seahorse Analyzer.[43] Using a recently published method, we were able to perform a seahorse analysis on hfRPE grown directly on Transwells, allowing preservation of hfRPE polarity and differentiation during testing.[25] Figure 4C shows that neither ECAR nor OCR shift significantly in UAM-laden hfRPE cultures compared to those without UAM. As another marker of mitochondrial metabolism, RPE has recently been shown to undergo ketogenesis, with the ketone bodies secreted apically to metabolically support photoreceptors.[44,45] Interestingly, despite the lack of differences in mitochondrial metabolism by Seahorse analysis, we did find a small but significant decrease in ketogenesis in cultures with UAM (Fig. 4D). Secretion of ApoE or TIMP3 (Fig. 4E), key components of drusen, were no different between cultures with UAM (fed oxOS) and those without UAM (fed daily media changes). UAM also did not interrupt the polarity of cultures, as assessed by the preferentially basolateral secretion of TIMP3[46] and the preferentially apical secretion of PEDF[47] and ketone bodies[47] (Fig. 4F).

Despite the ability of hfRPE to tolerate UAM, accumulation did induce the mild impairment in ketogenesis detailed above (Fig. 4D) and alterations in expression of some, but not all, RPE differentiation markers (Fig. S3). In addition, UAM-laden hfRPE were less efficient at fully digesting a single regular OS bolus. While initial OS digestion rates were similar, UAM-laden hfRPE demonstrated longer retention of partially degraded rhodopsin fragments, as assessed by anti-rhodopsin antibodies targeting both rhodopsin C-terminus (1D4)[23] and N-terminus (MCA-B630)[22] (Fig. 5A). The rhodopsin C-terminus is cleaved early in the OS degradation process, and the N-terminus is cleaved late in degradation.[48] Given higher levels of both 1D4 and B630-labeled rhodopsin fragments in UAM-laden RPE, we conclude that UAM-induced phagocytic defects occur upstream in the OS degradative process.

Oxidative stress, drusen, and AMD may be associated with a senescent RPE phenotype,[49,50] and a variety of models of RPE stress induce a transition from a predominately epithelial phenotype to a mesenchymal state (epithelial-mesenchymal transition: EMT). EMT is associated with reduced photoreceptor support and eventual outer retinal degeneration.[51,52] In our UAM-laden hfRPE, even months after completion of oxOS feeding, there is markedly increased senescence, as assessed by beta-galactosidase activity staining (Fig. 5B). In certain small, rare patches of intense UAM-accumulation, cell morphology is rounded, pigmentation is altered, and cells appear to be migrating out of the monolayer. We term these patches "RPE clumps." They are seen only in our oxOS-fed cultures and stain positive with the EMT marker vimentin[53] (Fig. 5C). However, given the rarity of RPE clumps, EMT gene expression markers Slug and Twist1[54] are not meaningfully different in whole-well lysates from Transwells with and without UAM accumulation (Fig. 5D). Together, these results suggest that while hfRPE is remarkably resistant to deleterious effects from UAM accumulation, it does trigger subtle, ongoing phenotypic perturbation and stress, especially in the small areas where UAM accumulation is most intense.

Discussion

Whether lipofuscin is universally toxic to the RPE is hotly debated.[1,10,55] Lipofuscin accumulation is an invariant feature of aging RPE, but accumulation starts as early as a few years of age without producing RPE dysfunction. By midlife, the RPE contains substantial lipofuscin content,[56] but susceptibility to the prototypical RPE-degenerative disease, AMD, does not increase significantly until after 70 years of age.[57] This suggests that lipofuscin accumulation and RPE toxicity do not fully correlate. Conflicting data have been reported about the relationship of fundus autofluorescence (FAF), derived primarily from RPE lipofuscin, and AMD progression.[6,58,59] In other retinal degenerations, such as Stargardt disease, there may be a clearer correlation between FAF and degeneration.[60] Studying the relationship between FAF and degeneration in the clinic is fraught with difficulty. As the RPE degenerates, lipofuscin fluorophores are lost, even if they were initially toxic. Further, certain fluorophores may be photocleaved into toxic by-products, reducing fluorescence while actually increasing toxicity.[58]

To study lipofuscin toxicity in a more controlled setting, researchers have turned to cell culture models. The lipofuscin component A2E has been fed to a range of RPE culture models, with myriad toxic effects.[1,14] However, A2E represents only one component of lipofuscin, and its specific toxicity among numerous other components of lipofuscin is debated.[61] OS feeding to RPE cultures has the potential to more closely recapitulate the physiology of lipofuscinogenesis. While many groups have fed OS to a variety of cultured RPE models,[1] none have fed OS to low passage, well-differentiated primary human fetal RPE, which has emerged as a well-accepted model for in vivo RPE function.

Our initial attempts at repeated OS feeding to hfRPE cultures revealed a remarkable resistance to undigested autofluorescent material (UAM) accumulation, in contrast to ARPE-19 cells in this study and primary rabbit and human RPE culture models in the published literature.[1] This resistance suggests hfRPE possesses mechanisms for efficient phagocytosis, and these mechanisms are lost in other culture models. When UAM does accumulate, the phenotypic effects are mild. UAM had no impact on glycolysis or mitochondrial oxygen consumption rates, secretion of drusen components, cell polarity, or cell death.

UAM does cause a mild drop in trans-epithelial electrical resistance (TEER), ketogenesis, expression of certain but not all RPE differentiation markers, and OS degradative capacity, along with a dramatic increase in senescence. Each of these dysfunctions may be inconsequential to RPE survivability, but could lower the RPE's threshold for tolerating other age-related insults. For example, senescence is known to produce a chronic para-inflammatory environment that may be exacerbated by complement dysregulation seen in the AMD-susceptible CFH polymorphism.[62–64]

In small patches of our hfRPE cultures with intense UAM accumulation, EMT is apparent with pigment alteration, vimentin staining, and a mounded morphology that appears to be emerging from the cell monolayer. These areas of "RPE

Investigative Ophthalmology & Visual Science

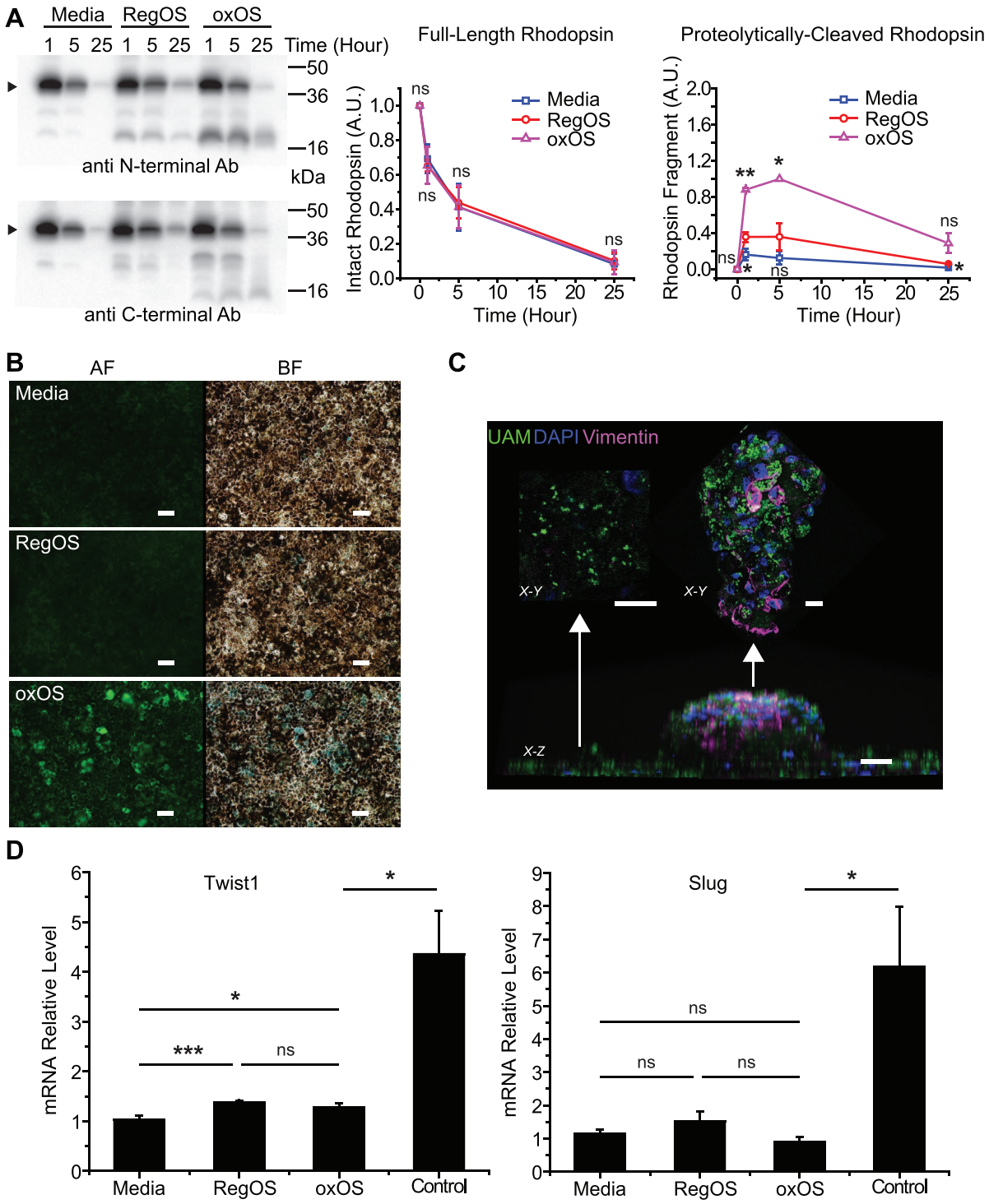

Figure 5. UAM induces mild phenotypic effects on hfRPE cultures. **(A)** Consumption of an OS bolus by hfRPE cultures previously fed oxOS to form UAM (oxOS) or previously fed RegOS or media only and therefore without UAM (RegOS, media). Amount of rhodopsin remaining in the combined supernatant plus cell lysate at 1, 5, and 25 hours after initiation of bolus. No OS washoff is performed, consistent with the "pulse-only" method outlined previously.[19] *Arrow* points to monomer band of rhodopsin. Smaller bands represent rhodopsin fragments, identified by N-terminal antibody B630 (*above*) and C-terminal antibody 1D4 (*below*). (*Right*) Quantification of monomer band rhodopsin shows no difference in consumption rates between conditions, but quantification of the main rhodopsin fragment recognized by B630 demonstrates higher formation rate and slower degradation of this fragment in hfRPE with UAM (oxOS); $n = 3$. **(B)** UAM-laden cultures (oxOS) have dramatically higher incidence of senescence than cultures previously fed RegOS or media only. AF, autofluorescence channel; BF, brightfield channel. Beta-galactosidase activity staining appears blue in BF channel. *Scale bar*: 50 µm. **(C)** Appearance of an "RPE clump," a rare focal area where UAM accumulation is particularly high. X-Z view demonstrates that the clump grows out of cell monolayer, although confocal analysis shows the clump is still a single cell layer thick. X-Y view from top of clump shows intense vimentin staining, whereas X-Y view from surrounding monolayer shows minimal vimentin staining. UAM (*green*), nuclei (*blue*), vimentin (*purple*). *Scale bar*: 20 µm. **(D)** qPCR demonstrates minimal differences in expression of EMT markers Twist1 or Slug in cultures with UAM (oxOS) versus without (RegOS, media), in contrast to controls. Control lysates are from hfRPE plated on plastic wells (rather than Transwells) at low density, conditions that encourage EMT. $n = 12$ for oxOS, RegOS, media conditions, $n = 5$ for control condition. $^{*}P < 0.05$, $^{**}P < 0.01$, $^{***}P < 0.001$.

Investigative Ophthalmology & Visual Science

clumping" may be analogous to the phenomenon of "cell extrusion" seen when unhealthy epithelial cells are pushed out of the epithelial monolayer while simultaneously undergoing EMT.[65] Interestingly, sick RPE cells migrate into the outer retina in AMD, seen clinically as hyperreflective foci above drusen and pigment epithelial detachments on optical coherence tomography (OCT).[66] Indeed, the morphology of our RPE clumps closely resembles the mushroom-like morphology of particular RPE cells in AMD patients that may ultimately slough and migrate to the outer retina.[3] The presence of these migrating RPE cells into the outer retina, as reflected by hyperreflective foci in the outer retina on OCT imaging, is predictive of progression of AMD to advanced stages.[67]

Initial UAM buildup in our cultures resulted in granules that were larger and spectrally blue-shifted from "native" lipofuscin granules measured from the RPE of aged humans without pathology. Interestingly, however, lipofuscin granules from AMD patients tend to be larger than those without AMD.[3] Further, the emission spectrum of these enlarged lipofuscin granules seen in AMD patients is not known. Over time, the UAM granules in our model system become smaller with a red-shift in their emission spectrum, more closely resembling the size and spectrum of lipofuscin granules from aged, non-pathologic human RPE. While entirely speculative, our in vitro data suggests the possibility that newly formed lipofuscin in vivo may initially have a larger granule size and blue-shifted emission spectrum, and as the lipofuscin granule compacts over time, it evolves into typical age-related lipofuscin. In AMD eyes, sick RPE may be less capable of efficiently compacting newly formed lipofuscin granules, leaving them larger, possibly with a blue-shifted emission spectrum, and possibly with more toxic properties than compacted lipofuscin.

Our study carries several limitations. While we showed that hfRPE is markedly resistant to UAM accumulation compared to the ARPE-19 RPE cell line, we did not directly test the resistance of other primary RPE culture models in this study. Instead, when we subjected hfRPE to the same (or more intense) OS feeding regimens as prior studies that demonstrated UAM accumulation in animal or human primary RPE cultures, we found no UAM buildup, implying hfRPE is also more resistant to UAM buildup than other primary RPE culture models. An additional limitation of our study is that feeding photo-oxidized OS to RPE cells in culture may alter the more natural process of slow lipofuscinogenesis that would occur with feeding unaltered OS. Further, the emission spectrum of initially accumulated UAM is blue-shifted from the spectrum seen in lipofuscin-laden RPE taken from healthy, older humans, although the UAM spectrum evolves over time in culture to more closely resemble native lipofuscin. While the composition of UAM and in vivo lipofuscin likely do not completely overlap, the goal of our study was to understand how highly differentiated, healthy RPE adapts to the continued accumulation of undigested, oxidized, lipid-rich granules. Each component of lipofuscin may have a particular toxicity and some components may be present or absent from our UAM-model, but it was our intent to understand how the aggregated mixture of lipofuscin-like material may alter RPE physiology. By utilizing an in vitro system, we are able to comment on the adaptation of RPE to lipofuscin-like material in ways not available by in vivo analysis, including the longitudinal tracking of granules over nearly a year.

In conclusion, well-differentiated, highly polarized primary human fetal RPE cultures are remarkably impervious to UAM build-up. The mechanisms of this resistance are under active investigation. Further, hfRPE is resistant to overt toxicity when UAM does accumulate. This resistance may help explain the conflicting reports in the literature on lipofuscin toxicity. Healthy RPE, such as hfRPE cultures, may be highly adaptable to lipofuscin accumulation, and detrimental effects may only manifest when the RPE experiences additional stressors.

Acknowledgments

Supported by the Kellogg Eye Center Pre-Residency Fellowship Program. Additional private grants were received from Barbara Dunn and from the Wayne and Shelly Jones Family Foundation; NEI Training Grant T32EY20485 (MAC); and NEI Grant R01EY025790 (DV). This work utilized the Vision Research Core funded by P30 EY007003 from the National Eye Institute. Electron microscopy was performed at the Michigan Medicine BRCF Microscopy Core with help from Aaron Taylor, Linda Barthel, and Jeff Harrison. Statistical analysis of Seahorse data using mixed effects models was performed with help from Consulting for Statistics, Computing and Analytics Research (CSCAR) at the University of Michigan.

Disclosure: **Q. Zhang**, None; **F. Presswalla**, None; **M. Calton**, None; **C. Charniga**, None; **J. Stern**, None; **S. Temple**, None; **D. Vollrath**, None; **D.N. Zacks**, None; **R.R. Ali**, None; **D.A. Thompson**, None; **J.M.L. Miller**, None

References

1. Boulton ME. Studying melanin and lipofuscin in RPE cell culture models. *Exp Eye Res*. 2014;126:61–67.
2. Ach T, Huisingh C, McGwin G, et al. Quantitative autofluorescence and cell density maps of the human retinal pigment epithelium. *Invest Ophthalmol Vis Sci*. 2014;55:4832–4841.
3. Ach T, Tolstik E, Messinger JD, Zarubina AV, Heintzmann R, Curcio CA. Lipofuscin redistribution and loss accompanied by cytoskeletal stress in retinal pigment epithelium of eyes with age-related macular degeneration. *Invest Ophthalmol Vis Sci*. 2015;56:3242–3252.
4. Feeney-Burns L, Hilderbrand ES, Eldridge S. Aging human RPE: morphometric analysis of macular, equatorial, and peripheral cells. *Invest Ophthalmol Vis Sci*. 1984;25:195–200.
5. Ng K-P, Gugiu B, Renganathan K, et al. Retinal pigment epithelium lipofuscin proteomics. *Mol Cell Proteomics MCP*. 2008;7:1397–1405.
6. Gliem M, Müller PL, Finger RP, McGuinness MB, Holz FG, Charbel Issa P. Quantitative fundus autofluorescence in early and intermediate age-related macular degeneration. *JAMA Ophthalmol*. 2016;134:817–824.
7. Sparrow JR, Dowling JE, Bok D. Understanding RPE lipofuscin. *Invest Ophthalmol Vis Sci*. 2013;54:8325–8326.
8. Lenis TL, Hu J, Ng SY, et al. Expression of ABCA4 in the retinal pigment epithelium and its implications for Stargardt macular degeneration. *Proc Natl Acad Sci U S A*. 2018;115:E11120–E11127.
9. Sparrow JR. Bisretinoids of RPE lipofuscin: trigger for complement activation in age-related macular degeneration. In: Lambris JD, Adamis AP, eds. *Inflammation and Retinal Disease: Complement Biology and Pathology. Advances in Experimental Medicine and Biology*. New York: Springer; 2010:63–74.
10. Sparrow JR, Boulton M. RPE lipofuscin and its role in retinal pathobiology. *Exp Eye Res*. 2005;80:595–606.
11. Smith RT. Quantitative fundus autofluorescence—Reply. *JAMA Ophthalmol*. 2017;135:403–404.
12. Wang Y, Kim HJ, Sparrow JR. Quercetin and cyanidin-3-glucoside protect against photooxidation and photodegradation of A2E in retinal pigment epithelial cells. *Exp Eye Res*. 2017;160:45–55.
13. Holz FG, Schütt F, Kopitz J, et al. Inhibition of lysosomal degradative functions in RPE cells by a retinoid component of lipofuscin. *Invest Ophthalmol Vis Sci*. 1999;40:737–743.
14. Kaur G, Tan LX, Rathnasamy G, et al. Aberrant early endosome biogenesis mediates complement activation in the retinal

pigment epithelium in models of macular degeneration. *Proc Natl Acad Sci U S A*. 2018;115:9014–9019.

15. Adler L, Boyer NP, Anderson DM, et al. Determination of N-retinylidene-N-retinylethanolamine (A2E) levels in central and peripheral areas of human retinal pigment epithelium. *Photochem Photobiol Sci*. 2015;14:1983–1990.
16. Brandstetter C, Holz FG, Krohne TU. Complement component c5a primes retinal pigment epithelial cells for inflammasome activation by lipofuscin-mediated photooxidative damage. *J Biol Chem*. 2015;290:31189–31198.
17. Pfeffer BA, Philp NJ. Cell culture of retinal pigment epithelium: Special Issue. *Exp Eye Res*. 2014;126:1–4.
18. Dunn KC, Aotaki-Keen AE, Putkey FR, Hjelmeland LM. ARPE-19, a human retinal pigment epithelial cell line with differentiated properties. *Exp Eye Res*. 1996;62:155–169.
19. Zhang Q, Presswalla F, Feathers K, et al. A platform for assessing outer segment fate in primary human fetal RPE cultures. *Exp Eye Res*. 2018;178:212–222.
20. Blenkinsop TA, Saini JS, Maminishkis A, et al. Human adult retinal pigment epithelial stem cell-derived RPE monolayers exhibit key physiological characteristics of native tissue. *Invest Ophthalmol Vis Sci*. 2015;56:7085–7099.
21. Blenkinsop TA, Salero E, Stern JH, Temple S. The culture and maintenance of functional retinal pigment epithelial monolayers from adult human eye. *Methods Mol Biol Clifton NJ*. 2013;945:45–65.
22. Röhlich P, Adamus G, Hugh McDowell J, Hargrave PA. Binding pattern of anti-rhodopsin monoclonal antibodies to photoreceptor cells: an immunocytochemical study. *Exp Eye Res*. 1989;49:999–1013.
23. Molday RS. Monoclonal antibodies to rhodopsin and other proteins of rod outer segments. *Prog Retin Res*. 1988;8:173–209.
24. Bligh EG, Dyer WJ. A rapid method of total lipid extraction and purification. *Can J Biochem Physiol*. 1959;37:911–917.
25. Calton MA, Beaulieu MO, Benchorin G, Vollrath D. Method for measuring extracellular flux from intact polarized epithelial monolayers. *Mol Vis*. 2018;24:425–433.
26. Bates D, Mächler M, Bolker B, Walker S. Fitting linear mixed-effects models using lme4. *J Stat Softw*. 2015;67:1–48.
27. Hothorn T, Bretz F, Westfall P. Simultaneous inference in general parametric models. *Biom J Biom Z*. 2008;50:346–363.
28. Yu L, Liu S, Guo W, et al. hTERT promoter activity identifies osteosarcoma cells with increased EMT characteristics. *Oncol Lett*. 2014;7:239–244.
29. Asnaghi L, Gezgin G, Tripathy A, et al. EMT-associated factors promote invasive properties of uveal melanoma cells. *Mol Vis*. 2015;21:919–929.
30. Karakashev S, Zhu H, Wu S, et al. CARM1-expressing ovarian cancer depends on the histone methyltransferase EZH2 activity. *Nat Commun*. 2018;9:631.
31. Peng S, Rao VS, Adelman RA, Rizzolo LJ. Claudin-19 and the barrier properties of the human retinal pigment epithelium. *Invest Ophthalmol Vis Sci*. 2011;52:1392–1403.
32. Boulton M, McKechnie NM, Breda J, Bayly M, Marshall J. The formation of autofluorescent granules in cultured human RPE. *Invest Ophthalmol Vis Sci*. 1989;30:82–89.
33. Sundelin SP, Nilsson SE. Lipofuscin-formation in retinal pigment epithelial cells is reduced by antioxidants. *Free Radic Biol Med*. 2001;31:217–225.
34. Zhang L, Hui Y-N, Wang Y-S, Ma J-X, Wang J-B, Ma L-N. Calcium overload is associated with lipofuscin formation in human retinal pigment epithelial cells fed with photoreceptor outer segments. *Eye*. 2011;25:519–527.
35. Mazzoni F, Safa H, Finnemann SC. Understanding photoreceptor outer segment phagocytosis: use and utility of RPE cells in culture. *Exp Eye Res*. 2014;126:51–60.
36. Bergmann M, Schütt F, Holz FG, Kopitz J. Inhibition of the ATP-driven proton pump in RPE lysosomes by the major lipofuscin fluorophore A2-E may contribute to the pathogenesis of age-related macular degeneration. *FASEB J*. 2004;18:562–564.
37. Wihlmark U, Wrigstad A, Roberg K, Brunk UT, Nilsson SE. Formation of lipofuscin in cultured retinal pigment epithelial cells exposed to pre-oxidized photoreceptor outer segments. *APMIS Acta Pathol Microbiol Immunol Scand*. 1996;104:272–279.
38. Bazan HE, Bazan NG, Feeney-Burns L, Berman ER. Lipids in human lipofuscin-enriched subcellular fractions of two age populations. Comparison with rod outer segments and neural retina. *Invest Ophthalmol Vis Sci*. 1990;31:1433–1443.
39. Pollreisz A, Messinger JD, Sloan KR, et al. Visualizing melanosomes, lipofuscin, and melanolipofuscin in human retinal pigment epithelium using serial block face scanning electron microscopy. *Exp Eye Res*. 2018;166:131–139.
40. Biesemeier A, Schraermeyer U, Eibl O. Chemical composition of melanosomes, lipofuscin and melanolipofuscin granules of human RPE tissues. *Exp Eye Res*. 2011;93:29–39.
41. Kennedy CJ, Rakoczy PE, Constable IJ. Lipofuscin of the retinal pigment epithelium: a review. *Eye*. 1995;9:763–771.
42. Lamming DW, Bar-Peled L. Lysosome: the metabolic signaling hub. *Traffic*. 2019;20:27–38.
43. Adijanto J, Philp NJ. Cultured primary human fetal retinal pigment epithelium (hfRPE) as a model for evaluating RPE metabolism. *Exp Eye Res*. 2014;126:77–84.
44. Adijanto J, Du J, Moffat C, Seifert EL, Hurley JB, Philp NJ. The retinal pigment epithelium utilizes fatty acids for ketogenesis implications for metabolic coupling with the outer retina. *J Biol Chem*. 2014;289:20570–20582.
45. Reyes-Reveles J, Dhingra A, Alexander D, Bragin A, Philp NJ, Boesze-Battaglia K. Phagocytosis dependent ketogenesis in retinal pigment epithelium. *J Biol Chem*. 2017;292:8038–8047.
46. Galloway CA, Dalvi S, Hung SSC, et al. Drusen in patient-derived hiPSC-RPE models of macular dystrophies. *Proc Natl Acad Sci U S A*. 2017;114:E8214–E8223.
47. Maminishkis A, Chen S, Jalickee S, et al. Confluent monolayers of cultured human fetal retinal pigment epithelium exhibit morphology and physiology of native tissue. *Invest Ophthalmol Vis Sci*. 2006;47:3612–3624.
48. Esteve-Rudd J, Lopes VS, Jiang M, Williams DS. In vivo and in vitro monitoring of phagosome maturation in retinal pigment epithelium cells. *Adv Exp Med Biol*. 2014;801:85–90.
49. Mishima K, Handa JT, Aotaki-Keen A, Lutty GA, Morse LS, Hjelmeland LM. Senescence-associated beta-galactosidase histochemistry for the primate eye. *Invest Ophthalmol Vis Sci*. 1999;40:1590–1593.
50. Zhu D, Wu J, Spee C, Ryan SJ, Hinton DR. BMP4 Mediates oxidative stress-induced retinal pigment epithelial cell senescence and is overexpressed in age-related macular degeneration. *J Biol Chem*. 2009;284:9529–9539.
51. Datta S, Cano M, Ebrahimi K, Wang L, Handa JT. The impact of oxidative stress and inflammation on RPE degeneration in non-neovascular AMD. *Prog Retin Eye Res*. 2017;60:201–218.
52. Zhao C, Yasumura D, Li X, et al. mTOR-mediated dedifferentiation of the retinal pigment epithelium initiates photoreceptor degeneration in mice. *J Clin Invest*. 2011;121:369–383.
53. Tamiya S, Liu L, Kaplan HJ. Epithelial-mesenchymal transition and proliferation of retinal pigment epithelial cells initiated upon loss of cell-cell contact. *Invest Ophthalmol Vis Sci*. 2010;51:2755–2763.
54. Díaz V, Viñas-Castells R, García de Herreros A. Regulation of the protein stability of EMT transcription factors. *Cell Adhes Migr*. 2014;8:418–428.

Investigative Ophthalmology & Visual Science

55. Rudolf M, Vogt SD, Curcio CA, et al. Histologic basis of variations in retinal pigment epithelium autofluorescence in eyes with geographic atrophy. *Ophthalmology*. 2013;120: 821–828.
56. Wing GL, Blanchard GC, Weiter JJ. The topography and age relationship of lipofuscin concentration in the retinal pigment epithelium. *Invest Ophthalmol Vis Sci*. 1978;17: 601–607.
57. la Cour M, Kiilgaard JF, Nissen MH. Age-related macular degeneration. *Drugs Aging*. 2002;19:101–133.
58. Sparrow JR. Quantitative fundus autofluorescence. *JAMA Ophthalmol*. 2017;135:403–403.
59. Zanzottera EC, Ach T, Huisingh C, Messinger JD, Spaide RF, Curcio CA. Visualizing retinal pigment epithelium phenotypes in the transition to geographic atrophy in age-related macular degeneration. *Retina Phila Pa*. 2016;36(suppl 1):S12–S25.
60. Sparrow JR. Light come shining: fundus autofluorescence. *J Pediatr Ophthalmol Strabismus*. 2018;55:285–286.
61. Smith RT, Bernstein PS, Curcio CA. Rethinking A2E. *Invest Ophthalmol Vis Sci*. 2013;54:5543–5543.
62. Daiger SP. Was the human genome project worth the effort? *Science*. 2005;308:362–364.
63. Kozlowski MR. RPE cell senescence: a key contributor to age-related macular degeneration. *Med Hypotheses*. 2012;78:505–510.
64. Chen M, Xu H. Parainflammation, chronic inflammation and age-related macular degeneration. *J Leukoc Biol*. 2015;98: 713–725.
65. Ohsawa S, Vaughen J, Igaki T. Cell extrusion: a stress-responsive force for good or evil in epithelial homeostasis. *Dev Cell*. 2018;44:284–296.
66. Balaratnasingam C, Messinger JD, Sloan KR, Yannuzzi LA, Freund KB, Curcio CA. Histologic and optical coherence tomographic correlates in drusenoid pigment epithelium detachment in age-related macular degeneration. *Ophthalmology*. 2017;124:644–656.
67. Christenbury JG, Folgar FA, O'Connell RV, Chiu SJ, Farsiu S, Toth CA. Progression of intermediate age-related macular degeneration with proliferation and inner retinal migration of hyperreflective foci. *Ophthalmology*. 2013;120:1038–1045.

Investigative Ophthalmology & Visual Science